Physical Processes in Hollow Cathodes

M. Krishnan,* R. G. Jahn,† W. F. von Jaskowsky,‡ and K. E. Clark§
Princeton University, Princeton, N.J.

Hollow cathodes with cavity diameters of 1.9 cm have been operated in an MPD arc configuration at discharge currents from 0.25 kA to 30 kA. Current and potential distributions, measured with probes in the cathode cavity, show that a spontaneous mode of hollow cathode operation, wherein the current distribution penetrates upstream into the cavity, has been achieved for particular combinations of discharge current and mass flows. These measured distributions are consistent with a conduction model which suggests that maximum current penetration, and the more efficient cathode emission which accompanies it, occurs when the dominant mean free path for electron energy exchange is comparable to the cavity diameter.

Introduction

HOLLOW cathodes were first used to advantage by Paschen for spectroscopic studies where they were shown to be capable of simultaneously providing high electron number density and relatively low ion and neutral temperatures in an essentially field-free cavity.[1] More recently, hollow cathodes have been studied extensively as sources of dense, highly ionized plasmas for a variety of purposes.[2,3] Typically, these provide plasmas of high electron density, high degrees of ionization, and low contamination by cathode material. Hollow cathodes also are used as electron emitters in advanced ion thrusters, where they exhibit longer lifetime and greater reliability than oxide-coated or liquid metal cathodes.[4]

Despite their broad utility, the physical processes inside hollow cathodes are still poorly understood. The inherently complex interaction between the plasma and the cavity walls does not lend itself to empirical modeling, and microscopic data on the plasma properties are sparse. One of the principal hindrances to detailed diagnostics is the typically small dimensions of the usual cavities—at most a few millimeters —which precludes access by probes to the cavity plasma and severely restricts optical observation. Thus, the data necessary to identify the dominant processes of emission, ionization, and current conduction within the cavity are lacking.

The primary interest in hollow cathodes in this laboratory is in the context of high-power quasisteady magnetoplasmadynamic (MPD) accelerators for space propulsion and other applications.[5,6] At the power levels inherent in such devices, the arc dimensions predicate cathodes an order of magnitude larger than those typically employed in the previously referenced works, and hence, the first task of this program is to ascertain whether proper hollow cathode function can be extended to cavities of centimeter scale. If such operation can be achieved, however, a number of auxiliary benefits will derive, since these cavities are large enough to permit interior diagnostics of some resolution. Specifically, detailed experimental study of such large hollow cathodes may, by reasonable extrapolation and scaling, shed light on the operation of smaller units, such as the ion engine cathodes, which are not themselves directly accessible to such diagnosis. For example, the experimental studies described in this paper involve hollow cathodes of 1.9-cm i.d. operated at arc currents from 0.25 to 30 kA, and argon mass flows from 10^{-3} to 16 g/sec. Although these dimensions and currents are much higher than typical of low-current steady-state hollow cathodes of ion thrusters, the corresponding current densities and mass flux densities are commensurate, and, thus, there is some hope of scaling the results.

Presented as Paper 76-984 at the AIAA International Electric Propulsion Conference, Key Biscayne, Fla., Nov. 14-17, 1976; submitted Dec. 10, 1976; revision received June 2, 1977.

Index categories: Electric and Advanced Space Propulsion; Plasma Dynamics and MHD.

*Graduate Student; presently Applied Scientist, Mason Laboratory, Yale University, New Haven, Conn.

†Dean, School of Engineering and Applied Science. Fellow AIAA.

‡Senior Research Engineer and Lecturer. Member AIAA.

§Research Engineer. Member AIAA.

Experimental Apparatus

The quasisteady hollow cathode apparatus is shown schematically in Fig. 1. The cylindrical arc chamber is 12.7 cm in diameter × 5.1-cm deep, with the tungsten hollow cathode, described in detail later, located on the axis. The coaxial aluminum anode, 1.1-cm downstream of the cathode, has an orifice of 10.2-cm diam, an outer barrel diameter of 18.8 cm, and a thickness of 1 cm.

Argon propellant is injected into the discharge chamber at rates from 10^{-3} to 16 g/sec through a high-speed solenoid valve fed from a high-pressure reservoir. In this particular work, the gas enters the discharge chamber solely through the hollow cathode, although it could also be admitted through six outer injectors set in the insulating Plexiglas backplate, or through both.

Current to the discharge is supplied as a flat-topped pulse, typically of 1-msec duration, by an 84-station LC ladder network of 2200-μF total capacitance. When discharged through an adjustable impedance in series with the accelerator, this capacitor line is capable of providing currents from 0.25 to 30 kA.

The discharge plasma exhausts into a glass bell jar, 76-cm long × 45-cm i.d., evacuated to some 10^{-3} Torr prior to each

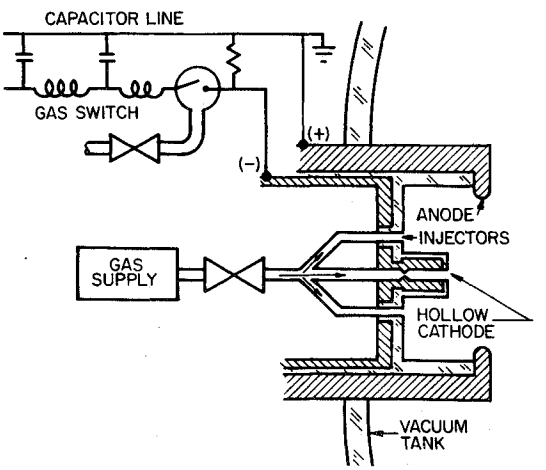

Fig. 1 Hollow cathode facility.

discharge by a mechanical pump. A probe carriage mounted inside the tank, controllable in two dimensions from outside, allows detailed probing both inside and outside the hollow cathode.

The magnetic field distribution within the cavity discharge is measured by a magnetic probe coil of 0.05-cm i.d. and 0.3-cm o.d., wound from 350 turns of No. 44 magnet wire. The probe signal is passively integrated and displayed on a Tektronix 551 oscilloscope. This recorded magnetic field is proportional to the enclosed current within the radius of the probe position, so that the radial current density is derivable from the slope of the magnetic field relative to the axial coordinate. At very low currents, the small signal from the integrator is boosted by a differential amplifier. Plasma floating potentials inside the cavity are mapped by a single Langmuir probe, consisting of a cylindrical tungsten wire 0.025 cm in diameter, imbedded in a quartz tube of 0.16-cm o.d. with only the end face of the tungsten exposed to the plasma.

Hollow Cathode Operation

If the outer surface of the hollow cathode is left uninsulated, there is no guarantee that the current will attach only in the cavity, a condition presumed to yield the most efficient cathode operation. Indeed, preliminary tests with uninsulated hollow cathodes showed that, for most operating conditions, a preference for attachment on the outer surface was displayed, regardless of cathode length, diameter, or cross-sectional variation.[7] Consequently, as a first step in the study of current conduction processes inside the hollow cathode, the outer barrel and end face of a straight cylindrical hollow cathode were insulated as shown in Fig. 2. The only cathode surface thus left exposed to the discharge was a 1.9-cm-i.d. × 3.2-cm-long tungsten cavity and the short molybdenum nozzle which feeds argon propellant to it.

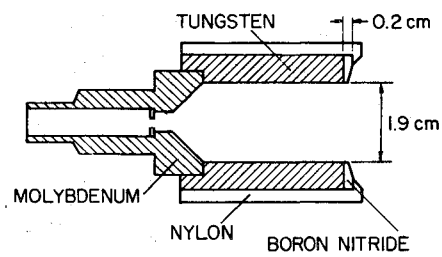

Fig. 2 Hollow cathode configuration.

Current and potential distributions inside this cathode cavity were determined over a range of currents and mass flows of 0.25-17 kA and 10^{-3}-8 g/sec of argon, respectively. Figure 3 shows the surface current density profiles for various mass flows from 5×10^{-3} to 0.4 g/sec at a discharge current of 0.25 kA. Three characteristic features may be noted:

1) As the mass flow is reduced from 0.4 to 0.1 g/sec, the peak in the surface current density distribution moves from 0.3 to 1.9 cm upstream of the cathode orifice.

2) Over this same range in mass flow, the length of the cathode over which 80% of the input current is found to attach to the surface increases from 0.7 to 2.2 cm, i.e., the current attachment at the surface becomes more diffuse.

3) Further reduction in mass flow from 10^{-1} to 5×10^{-3} g/sec causes the peak in the current distribution to move back downstream toward the open end of the cavity.

Figure 4 shows surface current density profiles for a higher current of 0.9 kA and mass flows from 5×10^{-3} to 8 g/sec. Here, just as at 0.25 kA, the current density peak first moves upstream from the cavity orifice and the current attachment becomes more diffuse as the mass flow is reduced from 8 to 6.6×10^{-2} g/sec. With still further reduction in mass flow, from 6.6×10^{-2} to 5×10^{-3} g/sec, the peak current density again moves back downstream towards the cavity end. However, the maximum peak penetration at this higher current is only 0.9 cm, compared to 1.9 cm at 0.25 kA.

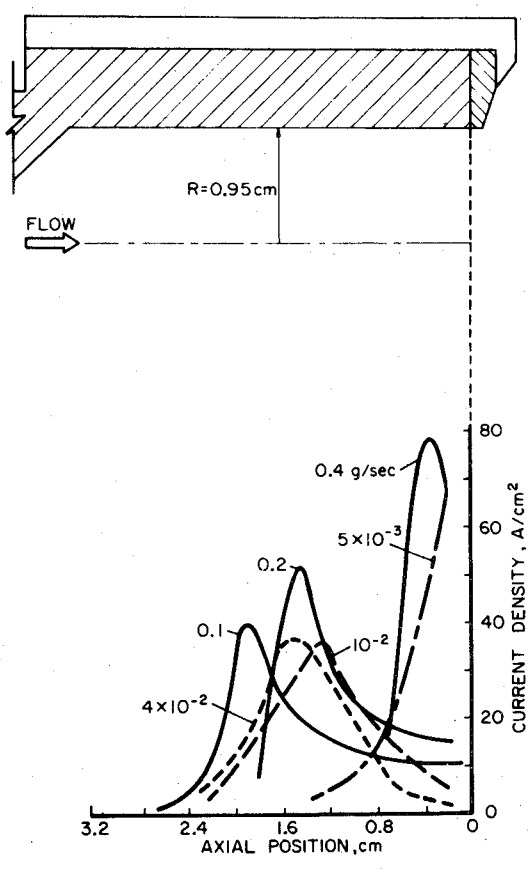

Fig. 3 Current density profiles, 0.25 kA.

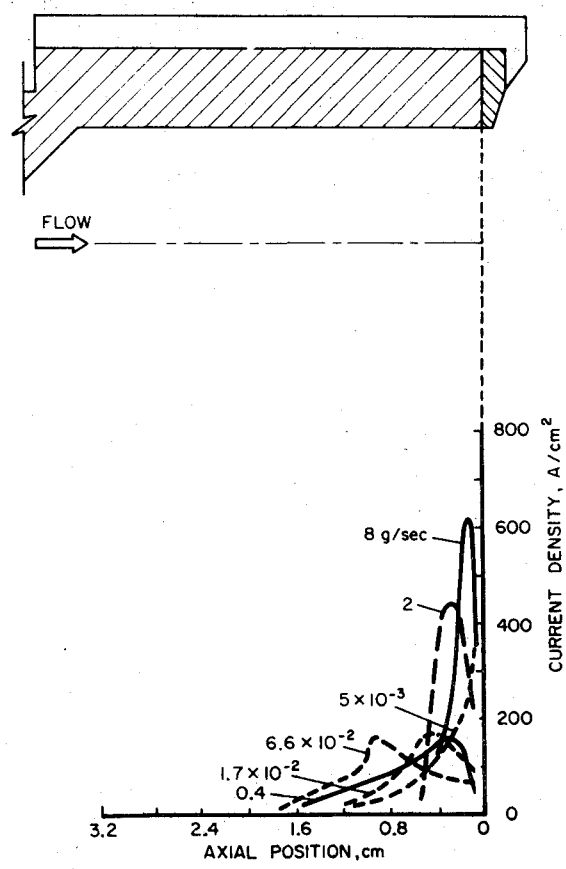

Fig. 4 Current density profiles, 0.9 kA.

Figure 5 shows similar surface current density distributions for a yet higher current of 4.7 kA. At this current the distributions are observed to be quite insensitive to changes in mass flow. For all mass flows, the peak current density occurs between 0 and 0.3 cm from the cavity orifice, and in all cases 80% of current attachment to the surface occurs over a length of 0.9 cm from the orifice.

The data presented in the preceding three figures may be cross plotted to demonstrate the effect of discharge current on the cavity current distribution. These distributions, shown in Fig. 6 for a mass flow of 0.2 g/sec, are normalized by the peak current density in each case to facilitate their comparison. As current is increased from 0.25 to 4.7 kA, the peak current density is seen to move nearer the cavity orifice, while current attachment occurs over shorter cathode channel lengths. To examine whether this trend continues to still higher currents, the surface current distribution was measured for a current of 16.7 kA. This distribution, also shown in Fig. 6, shows that the peak current density occurs still nearer the orifice, with only 0.8 cm of cathode length required for 80% current attachment to the surface.

To obtain information on the energy deposition inside the cavity, these surface current measurements were supplemented by more complete maps of magnetic field and floating potential throughout the cathode cavity for particular current and mass flow cases. Figure 7 shows, on a cross-sectional view of the cathode, solid line contours of constant current and dotted profiles of constant floating potential at a fixed current of 0.25 kA for mass flows of 0.4 and 0.1 g/sec. At this current, these mass flows produce extremes in the penetration of current into the cathode cavity. For both cases, the equipotential lines are approximately radial, implying a negligible radial field in most of the volume of the cavity. The axial field is also weak, something less than 4 V/cm. Since the cathode surface is the zero-volt equipotential, all of the radial equipotential contours must bend parallel to the surface somewhere close to it before leaving the cavity. If the potentials bend within the Debye sheath which separates the surface from quasineutral plasma, high radial fields of the order of 10^6 V/cm must exist at the surface. The implications of such fields for surface emission processes are discussed later.

From the intersecting grid of current and potential lines, the power density $j \cdot E$ deposited in different regions of the cavity plasma can be determined. The results of this computation are plotted in Fig. 8a for 0.4 g/sec and Fig. 8b for 0.1 g/sec. For both mass flows, the power density profiles near the surface are qualitatively similar to the current density profile measured at the same radial position. Furthermore, the power density profiles also reflect the deeper current penetration inferred earlier from the surface current density profiles in Fig. 3 when the mass flow was lowered from 0.4 to 0.1 g/sec.

Spontaneous Hollow Cathode Operation

The migration of the location of maximum surface current density upstream inside the cathode for certain combinations of discharge current and mass flow raises the question of whether the insulating covers placed around the barrel and end of the cathode to force the discharge inside are superfluous for those conditions. To test this criterion, the insulation on the face and outer surface of the hollow cathode was completely removed, and at operating conditions found earlier to favor penetration, the surface current distribution inside the cavity for this uninsulated cathode was measured. Some two thirds of the total discharge current was found to attach inside the cavity, distributed as shown by the solid line in Fig. 9. For comparison, the normalized current distribution for the insulated version of this cathode at the same current and mass flow is shown in the figure as the dashed line. The similarity between the two distributions demonstrates the spontaneous tendency of the cavity to carry the bulk of the arc current, even if its outer surfaces are available, provided the proper current and mass flow are selected.

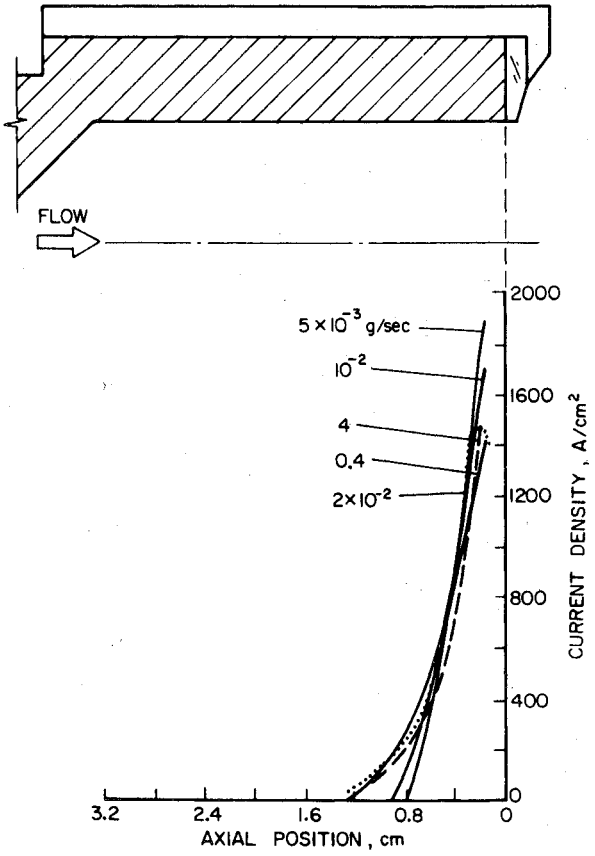

Fig. 5 Current density profiles, 4.7 kA.

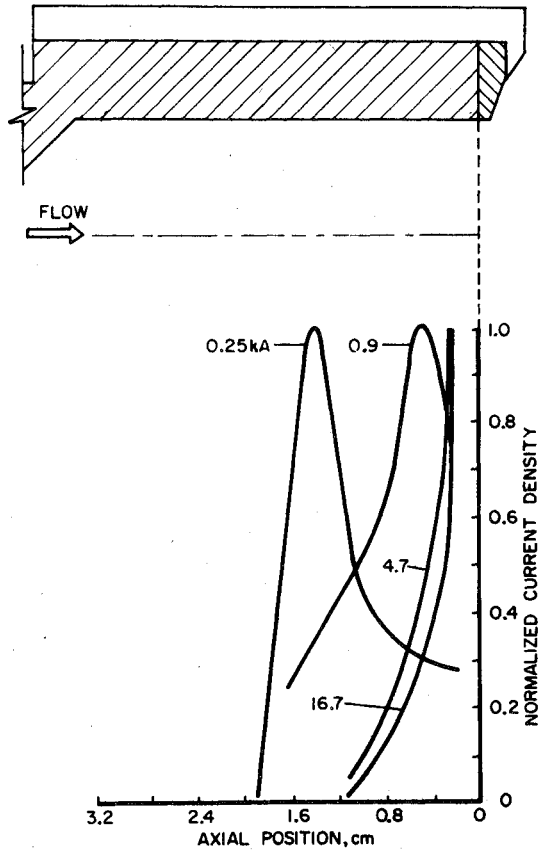

Fig. 6 Current density distributions, 0.2 g/sec.

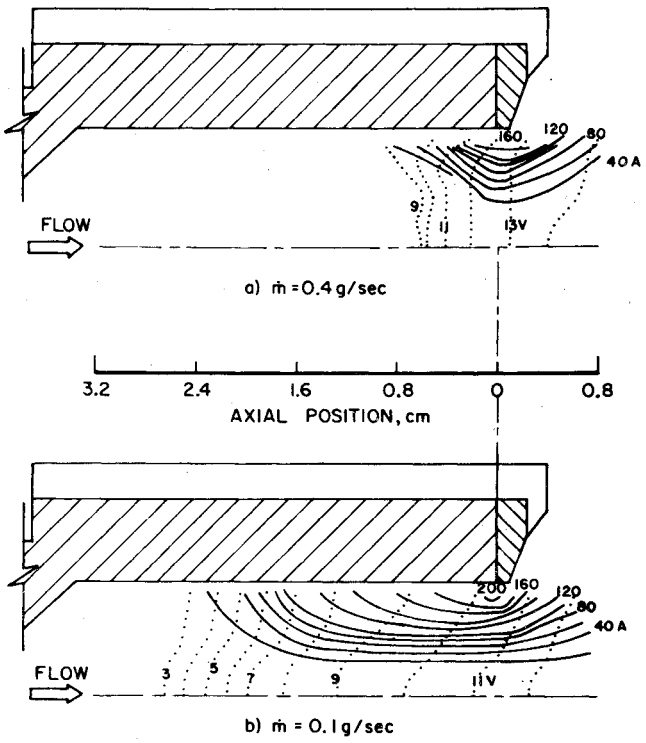

Fig. 7 Enclosed current and potential profiles, 0.25 kA.

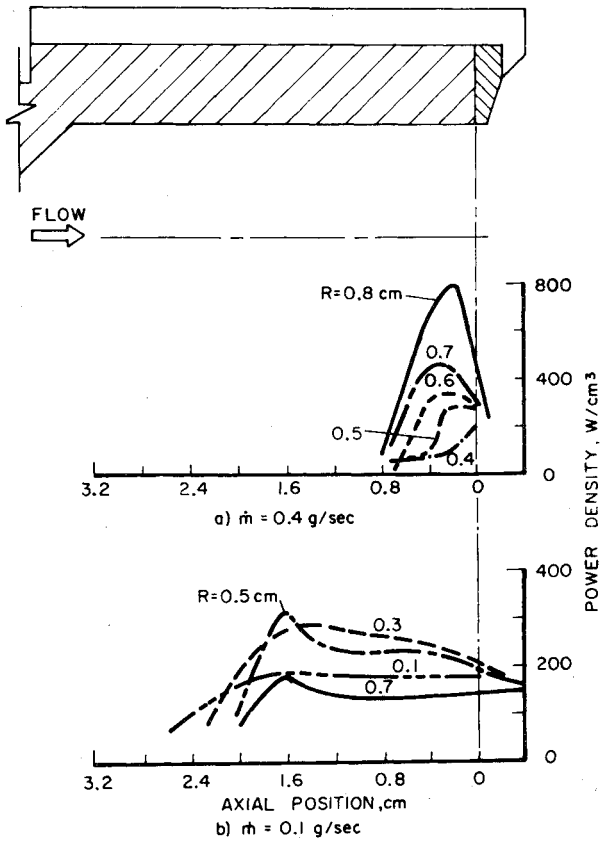

Fig. 8 Power density profiles, 0.25 kA.

Current Conduction Processes in the Hollow Cathode

As a first step in unraveling the cathode conduction process, the effect of mass flow was examined further to determine whether the static or dynamic head of the flowing gas is primarily responsible for governing the cavity current distributions. Several authors[2,3,8] favor the view that the static pressure of the flowing gas is the important factor, but none of these had the facility to verify this suggestion experimentally.

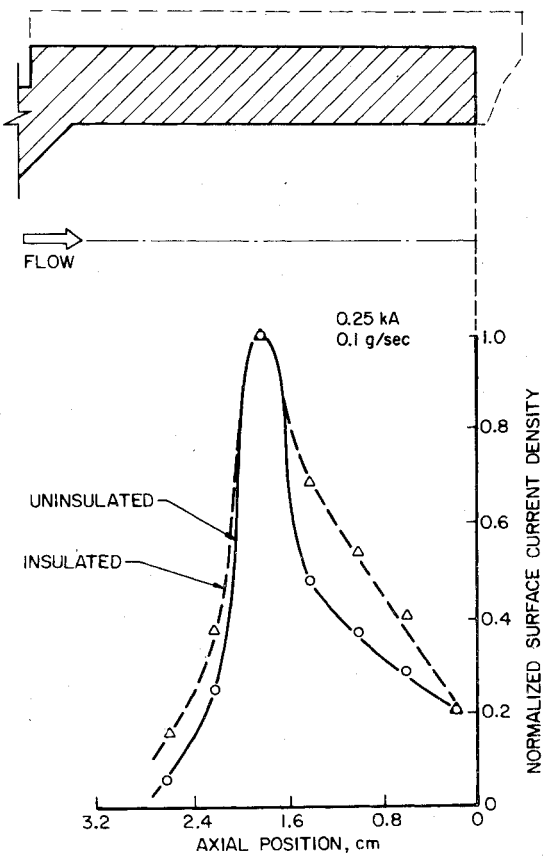

Fig. 9 Current density distributions.

For this experiment, gas flow to the hollow cathode was shut off completely, and the discharge vessel prefilled to various static pressures. The prefill pressures used in this experiment corresponded approximately to the static pressure component of the flowing gas in the earlier experiments with different mass flows, as estimated by a simplified gasdynamic analysis of the flow through the cathode[9]: a static pressure of 100 Torr corresponds to the highest mass flow of 0.4 g/sec, while a pressure of 0.05 Torr corresponds to the lowest mass flow of 5×10^{-3} g/sec.

The measured surface current distributions inside the hollow cathode are shown in Fig. 10 for a fixed current of 0.25 kA and several ambient prefill pressures. At 100 Torr the current density peak occurs near the cathode tip. At 5 Torr, the peak penetrates farther into the cavity and results in a more diffuse surface current attachment, just as with a reduction in mass flow from 0.4 to 0.1 g/sec as shown in Fig. 3. Further reduction in pressure from 5 Torr to 0.05 Torr causes the peak current density to move back toward the cathode tip as previously seen with the lowest mass flows. The observed similarity between the surface current distributions for different mass flows and for different ambient prefill pressures with no mass flow suggests that it is indeed the static pressure component of the flowing gas in the hollow cathode that determines the cavity current pattern.

The foregoing hypothesis further suggests that the cavity conduction is determined primarily by the "electrostatic" potential pattern. This suggestion is supported by an examination of the various terms in a generalized Ohm's Law[9] which indicates that induced fields due to mass motion of the plasma, electron pressure gradients, Hall effect, and ion slip are insignificant at all but extreme operating conditions of very high current (> 10 kA) and very low mass flow ($< 10^{-3}$ g/sec). If, in addition, the plasma conductivity could

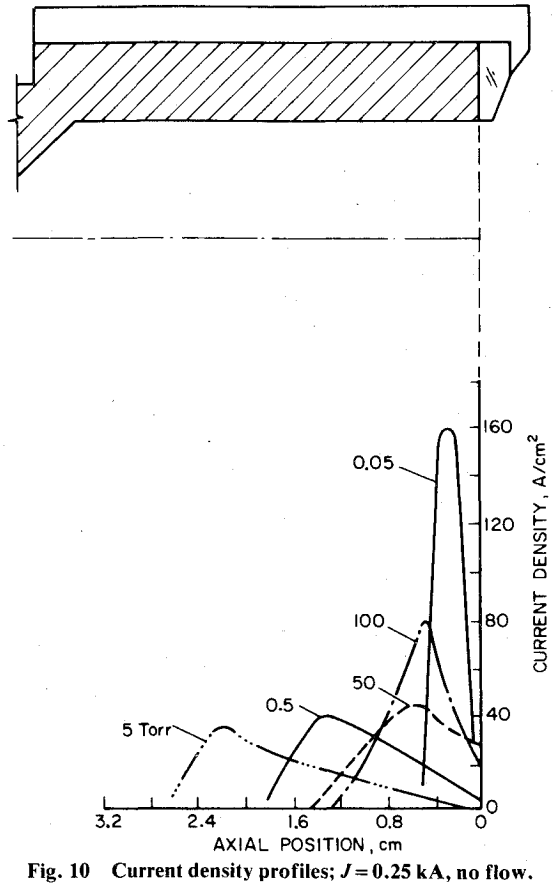

Fig. 10 Current density profiles; $J = 0.25$ kA, no flow.

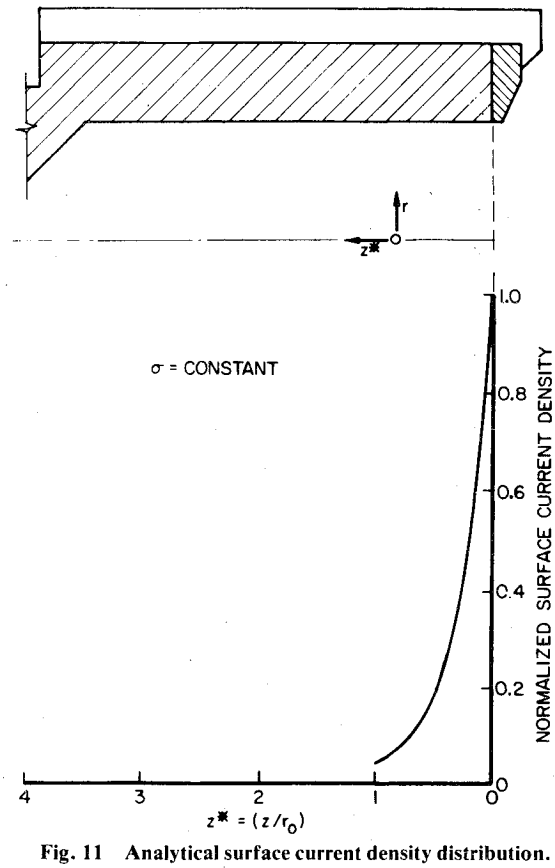

Fig. 11 Analytical surface current density distribution.

be presumed uniform within the cathode cavity, the potential would obey Laplace's equation, and the appropriate boundary value calculation would yield the potential field, and via this, the electric field and current density, everywhere inside the hollow cathode. Such an analytical current density distribution is shown in Fig. 11, and indicates that when the cathode current conduction is determined mainly by the electric field, the surface current density is highest at the orifice and 90% of the current entering the cathode attaches to the surface within an axial distance of less than one cathode radius upstream from the orifice. Comparison of this calculation with the experimentally observed distributions at higher currents (Fig. 5) indicates that in this range of currents, the "electrostatic" approximation is a good one.

However, this same model is inadequate for the "spontaneous" hollow cathode operation, where the peak current density occurs up to one diameter upstream of the orifice (Fig. 3, $\dot{m} = 0.1$ g/sec). Clearly the electric field does not dominate the distribution of current in this case; rather, the conductivity pattern in the cavity now seems to exert a major influence on the conduction pattern.

Detailed analysis of the conductivity in the cavity is beyond the scope of this effort, but a few qualitative arguments can be made. In general, the axial dependence of electron temperature, and hence of conductivity, must resemble one of the three profiles shown in the top row of Fig. 12. Far upstream of the cathode orifice, the cold entering gas is heated through an ionizing region up to a location at which the net energy input to the electron fluid is zero, i.e., the energy gained by electrons from the electric field is balanced by the loss of energy from electrons to heavy particles through elastic and inelastic scattering. From this axial location toward the cathode orifice, the conductivity remains constant until electron energy losses through the cavity orifice begin to be felt. More specifically, the escape of fast electrons from the orifice depresses the electron temperature, and hence the conductivity, over an axial extent related to the electron

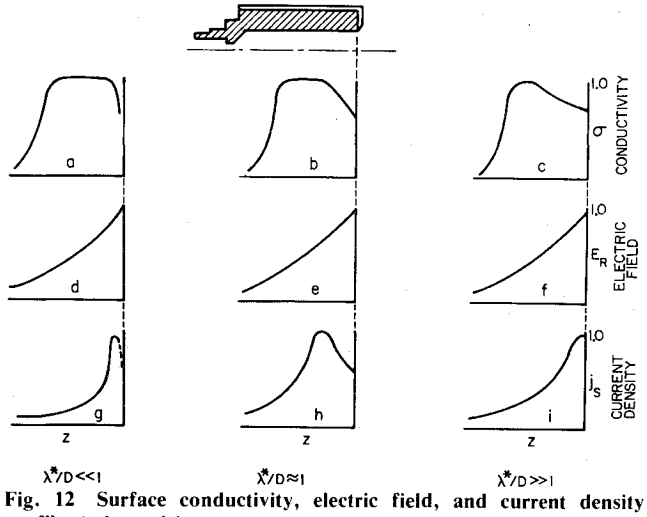

Fig. 12 Surface conductivity, electric field, and current density profiles (schematic).

energy-exchange mean free path. For the range of operating conditions used here, this mean free path λ^* can vary from a small fraction of the cathode diameter up to several cathode diameters.[9]

Figure 12 shows the qualitative effect on the axial conductivity in the cathode cavity of different values of λ^*. When $\lambda^* \ll D$, the cathode orifice diameter, the decrease in conductivity occurs only over a limited axial region near the orifice (Fig. 12a); when $\lambda^* \approx D$, the conductivity decrease extends about one diameter upstream of the orifice (Fig. 12b); and when $\lambda^* \gg D$, an electron a few diameters upstream of the tip has almost the same probability of escape as one nearer the cathode tip, resulting in a weak axial conductivity gradient over most of the cavity (Fig. 12c).

The surface current distributions to be expected in these situations follow from folding the conductivity profiles with

those of the applied electric field, shown for reference in the second row of Fig. 12. When $\lambda^* \ll D$, the conductivity gradient very near the orifice opposes the electric field gradient, and if strong enough to overbalance it, causes the peak current density to occur slightly upstream of the orifice (Fig. 12g). For $\lambda^* \approx D$, the product of conductivity and radial electric field produces a peak current density about one orifice diameter upstream of the peak (Fig. 12h). When $\lambda^* \gg D$, the rather weak conductivity gradient cannot overcome the electric field gradient, and the peak current density returns to the orifice (Fig. 12i).

In short, when the energy-exchange mean free path λ^* is either very small or very large compared to the cathode diameter, the resulting surface current distributions are roughly the same, and peak near the orifice. It is the intermediate case of $\lambda^* \approx D$ that results in attachment of the current peak upstream in the cavity. This simple model also predicts, however, that at best, the current can penetrate into the MPD hollow cathode to only the order of a cavity diameter.

Crude as it is, this model is consistent with the various experiments reported earlier; i.e., for any combination of current and mass flow, the observed cavity current distribution falls into the proper category for the prevailing λ^*/D, as calculated from the best estimates of the pertinent plasma properties.[9] For example, in Fig. 3, the 0.4 g/sec condition indeed involves a $\lambda^*/D \ll 1$, the 0.1 g/sec a $\lambda^*/D \approx 1$, and the 5×10^{-3} a $\lambda^*/D \gg 1$, etc. There is some hope, therefore, that $\lambda^*/D \approx 1$ is a generally serviceable criterion for spontaneous hollow cathode operation.

Some qualitative precedent for this argument is provided by certain glow discharge experiments in static helium and neon,[10] in which the discharge pressure, and therefore the energy-exchange mean free path, was fixed, and the hollow cathode diameter was varied. It was found that the most efficient discharge operation resulted at one particular cathode diameter; larger or smaller diameters produced inferior behavior. The discharge properties in the present arc experiments are, of course, quite different, but the λ^*/D mechanism may play much the same role.

Emission Processes at the Hollow Cathode Surface

The question of how the total discharge current is carried from the cathode metal through the cavity surface to the plasma in the cavity volume is also of considerable significance in understanding hollow cathode performance. To account for the emission of average current densities from several tens to more than 10^3 A/cm^2, thermionic emission would require surface temperatures far in excess of 2000 K, even for thoriated tungsten. However, a simple heat-transfer calculation[9] shows that the surface temperature of the cavity wall can rise only by a few hundred degrees Kelvin during the millisecond period of the quasisteady discharge, even if all of the discharge energy in the cavity were transferred to the cathode. Therefore, uniform thermionic emission cannot be considered to be the major source of charge carriers in the hollow cathode.

Field emission requires not only electric fields in excess of 10^6 V/cm, but also current densities larger than 10^7 A/cm^2.[11,13] Although electric fields of this magnitude may indeed exist next to the cathode surface over a Debye sheath of 10^{-5} cm, the simultaneous requirement on the magnitude of the current density exceeds the average experimental value by several orders of magnitude. Thus, uniform field emission must also be ruled out as a primary mechanism of current transfer at the cathode surface. It is possible that field emission may occur in a large number of intense "hot spots" on the surface, but this process could not be resolved by our experiments.

In the absence of demonstrated adequacy of thermionic or field emission, other processes need consideration; the most promising of these is photoelectric emission. Detailed analysis of this mechanism is beyond the scope of this paper, but it is relevant to summarize a related study.[14] To estimate whether the efficient containment of argon resonance radiation of AI and AII can account for a large part of the discharge current by photoelectric emission from the cavity wall, the cathode plasma was assumed fully ionized with all of the radiant energy in the cavity carried by 17-eV resonant photons of Ar II. The maximum possible flux of such resonant quanta to the surface was estimated by assuming that all of the cathode region power was invested in the radiation field. At the resonant wavelength ($\approx$723 Å), the maximum measured quantum yield (ejected electrons/incident quantum) for tungsten is about 0.2.[15] The product of the quantum flux and this maximum yield provides an upper bound to the vacuum photoelectric emission at the cathode surface. This maximum photo-emitted current density was shown to be between 25 and 50% of the measured average surface current density for all of the operating conditions examined. If instead of a fully ionized plasma, a weakly ionized plasma with all the radiant energy carried by 11.6-eV resonant quanta of Ar I were assumed, similar results were obtained. Photoelectric emission, possibly enhanced by large electric fields at the surface, has thus to be considered as a major source of charge carriers in the hollow cathode discharge.

Again there is some precedent for this hypothesis to be found in glow discharge research. The importance of photoelectric emission has long been recognized in hollow cathode glow discharges, which are copious sources of uv radiation.[16] For example, Little and von Engel[17] account for the hollow cathode effect in glow discharges in terms of a combination of enhanced electron current due to photoemission and enhanced ion current due to constriction of the cathode dark space.

Summary

The results and insight acquired in these experiments have been achieved with the most rudimentary hollow cathode system, i.e., a bare tungsten tube, in contrast to the hollow cathode systems used in ion engines, which require an array of supporting equipment, such as baffles, keepers, and low work function inserts. Although the roles of these appendages have not in any way been explored in this study, it seems reasonable to postulate that their function is to enforce profiles of electric potential and gas density similar to those found here to yield the best hollow cathode performance. Conversely, the present results suggest that this supporting equipment could be superfluous, even for low currents and mass flows where it typically is employed, if the hollow cathode dimensions were appropriately tailored to those conditions.

Acknowledgments

This work was supported by NASA Grant NGL 31-001-005. The authors wish to acknowledge the skillful laboratory assistance of A. Casini and D. Tregurtha.

References

[1] Paschen, F., *Annalen der Physik*, Vol. 50, 1916, p. 901.

[2] Lidsky, L. M., Rothleder, S. D., Rose, D. J., Yoshikawa, A., Michelson, C., and Mackin, R. J., Jr., "Highly Ionized Hollow Cathode Discharge," *Journal of Applied Physics*, Vol. 33, Aug. 1962, pp. 2490-2497.

[3] Delcroix, J-L. and Trindade, A. R., "Hollow Cathode Arcs," *Advances in Electronic and Electron Physics*, Vol. 35, edited by L. Marton, Academic Press, New York, 1974.

[4] Byers, D. C., "Performance of Various Oxide Magazine Cathodes on Kaufman Thrusters," NASA TN D-5074, 1968.

[5] Clark, K. E. and Jahn, R. G., "Quasi-steady Plasma Acceleration," *AIAA Journal*, Vol. 8, Feb. 1970, pp. 216-220.

[6] Rudolph, L. K., Jahn, R. G., Clark, K. E. and von Jaskowsky, W. F., "Performance Characteristics of Quasi-steady MPD Discharges," AIAA Paper 76-1000, Nov. 1976, Key Biscayne, Fla.

[7] Krishnan, M., Jahn, R. G., von Jaskowsky, W. F., and Clark, K. E., "Physical Processes in Hollow Cathodes," AIAA Paper 76-984, Nov. 1976, Key Biscayne, Fla.

[8] Minoo, H., "Gas-fed Hollow Cathode Arc Mechanisms," *Proceedings of 1st Interntional Conference on Hollow Cathode Discharges and Their Applications*, 1971, p. 15.

[9] Krishnan, M., "Physical Processes in Hollow Cathodes in High Current Discharges," Princeton University, Princeton, N.J., AMS Rept. 1293, July 1976.

[10] Sturges, D. J. and Oskam, H. J., "Studies of the Properties of the Hollow Cathode Glow Discharge in Helium and Neon," *Journal of Applied Physics*, Vol. 35, Oct. 1964, p. 2287.

[11] Mackeown, S. S., "The Cathode Drop in an Electric Arc," *Physical Review*, Vol. 34, 1929, p. 611.

[12] Fowler, R. H. and Nordheim, L. W., "Electron Emission in Intense Electric Fields," *Proceedings of the Royal Society, London*, Vol. A119, 1928, p. 173.

[13] Wasserab, T., "Zur Theorie des Quecksilber-Kathodenflecks," *Zeitschrift für Physik*, Vol. 130, 1951, p. 311.

[14] Krishnan, M., "On the Emission Mechanism in High Current Hollow Cathode Arcs," *Proceedings of Conference on Partially Ionized Plasmas Including the 3rd Symposium on Uranium Plasmas*, 1976, Princeton, N.J.

[15] Wheaton, J. E. G., "Photoelectric Yield of Tungsten," *Journal of the Optical Society of America*, Vol. 54, 1964, p. 287.

[16] Dauvillier, A., "Researches on the Electrical Discharge in Gases and the Accompanying Radiation," *Philosophical Magazine*, Vol. 2, 1926, p. 1046.

[17] Little, P. F. and von Engel, A., "The Hollow-Cathode Effect and the Theory of Glow Discharges," *Proceedings of the Royal Society, London*, Vol. A224, June 1954, p. 209.